Photochemistry and Photobiology, 2000, 72(4): 533–540

Scavenger-Receptor Targeted Photodynamic Therapy¶

Michael R. Hamblin*, Jaimie L. Miller and Bernhard Ortel

Wellman Laboratories of Photomedicine, Massachusetts General Hospital and Department of Dermatology, Harvard Medical School, Boston, MA

Received 26 April 2000; accepted 12 July 2000

ABSTRACT

Covalent conjugation of a photosensitizer to a ligand that specifically recognized and internalized by a cell-surface receptor may be a way of improving the selectivity of photodynamic therapy (PDT). The class A Type-I scavenger receptor of macrophages, which among other ligands recognizes maleylated serum albumin and has a high capacity is a good candidate for testing this approach. Chlorin$_{e6}$ was covalently attached to bovine serum albumin to give conjugates with molar substitution ratios of 1:1 and 3:1 (dye to protein), and these conjugates could then be further modified by maleylation. A novel way of purifying the conjugates by acetone precipitation was developed in order to remove traces of unbound dye that could not be accomplished by size-exclusion chromatography. Conjugates were characterized by polyacrylamide gel electrophoresis and thin-layer chromatography. Photosensitizer uptake was measured by target J774 murine macrophage-like cells and nontarget OVCAR-5 human ovarian cancer cells, and phototoxicity was examined after illumination by a 660 nm diode laser by a tetrazolium assay. All of the purified conjugates were taken up by and after illumination killed J774 cells while there was only small uptake and no phototoxicity toward OVCAR-5 cells. The higher dye:protein ratio and maleylation of the conjugates both produced higher uptakes and lower survival ratios in J774 cells. The uptake and phototoxicity by J774 cells were decreased after incubation at 4°C demonstrating internalization, and confocal microscopy with organelle-specific green fluorescent probes showed largely lysosomal localization. Uptake and phototoxicity by J774 cells could both be competed by addition of the scavenger receptor ligand maleylated albumin. These data show that scavenger receptor–targeted PDT gives a high degree of specificity toward macrophages and may have applications in the treatment of tumors and atherosclerosis.

INTRODUCTION

The targeting of drugs to desired cell types and tissues such as tumors may be improved by covalently attaching the drug molecule to ligands that bind to specific recognition sites such as antigens and receptors. Examples of these ligands include monoclonal antibodies (1), growth factors (2), peptides (3), hormones (4), vitamins (5) and lipoproteins (6). Depending on the nature of the drug targeted, there may be the necessity of the conjugate being internalized into tumor cells, and once internalized the conjugate may need to be degraded by intracellular enzymes to release the drug in an active form. The photosensitizers (PS)†; used in photodynamic therapy (PDT) have some selective accumulation in tumors, but since the mechanism of this selectivity is unknown (7), other ways of improving the tumor-targeting properties of PS are being sought. We have reported on the use of conjugates between PS and monoclonal antibodies (8–11), low-density lipoprotein (12) and transferrin (13). Others have described PS conjugates with different targeting agents including epidermal growth factor (14) and insulin (15).

In a previous study (13) we found that conjugates between bovine serum albumin (BSA) and the PS hematoporphyrin were recognized by the scavenger receptor of J774 mouse macrophage-like cell line. Macrophages and monocytes (and to a lesser extent endothelial cells) express several ''scavenger'' receptors which are membrane proteins that recognize a wide range of ligands, both naturally occurring and synthetic (16). Scavenger receptors are high capacity, lead to rapid endocytosis and subsequent routing to endosomes and lysosomes (17). The J774 murine macrophage cell line has been widely studied by workers investigating expression of scavenger receptors and targeting various drugs by conjugation to scavenger receptor ligands (18–20). Other workers have subsequently described the use of PS conjugates with maleylated serum albumin (a well-known scavenger receptor ligand [21]) to target phthalocyanines to J774 cells

¶Posted on the website on 8 August 2000.

*To whom correspondence should be addressed at: WEL 224, Wellman Laboratories of Photomedicine, Massachusetts General Hospital, 55 Fruit Street, Boston, MA 02114, USA. Fax: 617-726-3192, e-mail: hamblin@helix.mgh.harvard.edu

†*Abbreviations:* BSA, bovine serum albumin; c_{e6}, chlorin$_{e6}$; DMSO, dimethyl sulfoxide; EDTA, ethylenediamine-tetraacetic acid; FCS, fetal calf serum; HEPES, *N*-2-hydroxythylpiperazine-*N*′-2-ethane-sulfonic acid; mal, maleylated; MTT, 3-(4,5-dimethylthiazol-2-yl)-2,5-diphenyltetrazolium bromide; NHS, *N*-hydroxysuccinimide; PBS, phosphate-buffered saline; PDT, photodynamic therapy; PS, photosensitizer; R123, rhodamine 123; SDS, sodium dodecyl sulfate; SDS-PAGE; SDS polyacrylamide gel electrophoresis; TAM, tumor-associated macrophage; TLC, thin-layer chromatography.

(20), and there is also a report (22) of a maleylated serum albumin conjugate being used to target the photosensitizer chlorin$_{e6}$ (c_{e6}) to experimental intimal hyperplasia *in vivo*.

Tumor-associated macrophages (TAM) have been shown to play a major role in cancer growth (23). They produce mediators that increase the degree of angiogenesis (24,25), and both a poor prognosis (26) and occurrence of distant metastasis (27) have been correlated with the extent of macrophage infiltration of the tumors. It has been shown that the macrophage content of different tumors correlates well with the localization of PS (28) and that macrophages can accumulate several times more PS than tumor cells (29). The therapeutic tumor response to PDT can be dramatically potentiated by treatment with a macrophage activating factor (30) or a colony-stimulating factor (31). For these reasons the ability to specifically target PS to macrophages is of great interest.

In this report we describe the preparation of conjugates between BSA and the PS c_{e6} and their subsequent maleylation. A novel purification method using acetone precipitation allows sufficiently pure conjugates to provide specific targeting to scavenger receptor–positive J774 mouse macrophages, without uptake or phototoxicity to non–scavenger expressing tumor cells. Scavenger receptor targeting is demonstrated by competition of uptake and phototoxicity by maleylated (mal)-BSA, and internalization by comparing incubation at 37 and 4°C and two-color fluorescence confocal microscopy.

MATERIALS AND METHODS

Preparation of conjugates. Four conjugates were studied (2 BSA–c_{e6} conjugates and their maleylated counterparts). The *N*-hydroxy succinimide (NHS) ester of c_{e6} was prepared by reacting 1.5 equivalents of dicyclohexylcarbodiimide and 1.5 equivalents of NHS with 1 equivalent of c_{e6} (Porphyrin Products, Logan, UT) in dry dimethyl sulfoxide (DMSO). After standing in the dark at room temperature for 24 h the NHS ester was frozen in aliquots for further use. BSA (Sigma Chemical Co., St Louis, MO) (2×50 mg) was dissolved in $NaHCO_3$ buffer (0.1 *M*, pH 9.3, 3 mL) and 30 and 120 μL of c_{e6}–NHS ester added to respective tubes with vortex mixing. After being kept in the dark at room temperature for 6 h the crude conjugate preparations were each divided into two equal parts. One portion of each of the conjugate preparations was maleylated by adding solid maleic anhydride (20 mg) in portions to the protein preparation with vortex mixing and addition of saturated $NaHCO_3$ solution as needed to keep the pH above 7 (21). The reaction mixture was allowed to stand at room temperature in the dark for 3 h. Unmodified BSA was also maleylated to act as a control and as a competitor for the cellular uptake of conjugates.

Purification. Crude conjugate preparations (approximate concentration of protein 5 mg mL^{-1}) were added to 10× volume of acetone (ACS grade) slowly at 4°C, and were kept at 4°C for 6 h, followed by centrifugation at 4000 ***g*** for 15 min at 4°C. The supernatant was removed, and the pellet again suspended in the same volume of acetone and the centrifugation repeated. After each precipitation step the preparation was monitored by thin-layer chromatography (TLC). Up to five precipitation steps were necessary in order to completely remove noncovalently bound chlorin species. Finally the pellet was dissolved in 2 mL phosphate-buffered saline (PBS) and dialyzed twice against 20 L PBS overnight to remove traces of acetone. Sephadex G50 column chromatography was carried out by applying the reaction mixture from conjugation of 50 mg BSA with 5 mg c_{e6}-NHS ester to a 50×1 cm^2 Sephadex column that was eluted with PBS at 4°C. The absorbance of the eluted fractions was monitored at 400 nm and at 280 nm.

Characterization of conjugates. The concentrations of the constituents in the conjugates and hence the substitution ratios were measured by absorbance spectroscopy. An aliquot of the conjugate was diluted in 0.1 *M* NaOH/1% sodium dodecyl sulfate (SDS) and absorbance between 240 and 700 nm scanned. The extinction coefficient of BSA at 280 nm is 47 000 cm^{-1} *M*$^{-1}$ (32) while the extinction coefficient of c_{e6} at 400 nm is 150 000 cm^{-1} *M*$^{-1}$. TLC was performed on silica gel plates (Polygram SIL G/UV254, Macherey Nagel, Duren, Germany), the chromatograms were developed with a 1:1 mixture of 10% aqueous ammonium chloride and methanol, and spots were observed with fluorescence and absorbance imaging. SDS polyacrylamide gel electrophoresis (SDS-PAGE) was carried out essentially according to the method of Laemmli (33). Gradients of 4–10% acrylamide were used in a nonreducing gel and c_{e6} was localized on the gel by fluorescence excitation 400–440 nm bandpass filter, emission 580 longpass filter, (ChemiImager 4000, Alpha Innotech Corp, San Leandro, CA). Protein was localized by Coomassie blue staining.

Cellular uptake. J774.A1 (J774) mouse macrophage-like cell line was obtained from American Type Culture Collection (Rockville, MD). The National Institute of Health OVCAR-5 (OVCAR-5) human ovarian cancer cell line was obtained from Dr. T. Hamilton (Fox Chase Cancer Institute, Philadelphia, PA). Cells were grown in Roswell Park Memorial Institute 1640 media containing *N*-2-hydroxythylpiperazine-*N*′-2-ethane-sulfonic acid (HEPES), glutamine, 10% fetal calf serum (FCS), 100 U mL^{-1} penicillin and 100 μg mL^{-1} streptomycin. They were passaged by washing with PBS without Ca^{2+} and Mg^{2+}, and adding trypsin–ethylenediamine-tetraacetic acid (EDTA) to the plate for 10 min at 37°C.

Cells were grown to 90% confluency in 24-well plates and the conjugate or PS was added in 1 mL medium containing 10% serum to each well. The concentration range for the conjugates and free c_{e6} was between 0.5 and 4 μ*M* c_{e6} equivalent and the incubation time was 3 h. After incubation at 37°C, the medium was removed and cells were washed three times with 1 mL sterile PBS and incubated with 1 mL trypsin–EDTA for 20 min (OVCAR-5) or 60 min (J774). The cell suspension was then removed and centrifuged (5 min at 250 ***g***). The trypsin supernatant was aspirated and retained and the pellets (frequently visibly fluorescent under long wave UV) were dissolved in 1.5 mL of 0.1 *M* NaOH/1% SDS for at least 24 h to give a homogenous solution. The trypsin supernatant was checked for the presence of fluorescence to quantify any surface binding which might easily be removed by trypsin. The fluorescence was measured using an excitation wavelength of 400 nm and the emission scanned from 580 to 700 nm in order to calculate the peak area (λ_{max} = 664 nm). A series of dilutions in 1.5 mL 0.1 *M* NaOH/1% SDS of known concentrations of each separate conjugate and PS was scanned for fluorescence as above in order to prepare calibration curves to allow quantitation of the c_{e6} by conversion of the measured peak areas into mol c_{e6} equivalent. The protein content of the entire cell extract was then determined by a modified Lowry method (34) using BSA dissolved in 0.1 *M* NaOH/1% SDS to construct calibration curves. Results were expressed as mol of c_{e6} per mg cell protein. For measuring the cellular uptake at 4°C, precooled growth media was used and the plates with cells were cooled to 4°C in an ice-bath for 20 min before the addition of PS solutions as well as after the addition. The incubation was carried out in the normal atmosphere in the dark (plates wrapped in aluminum foil).

PDT studies. Cells were seeded in 24-well plates, at densities of 100 000 cells in 1 mL medium. After 24 h, the cells were given 1 mL fresh medium containing 10% serum and a specific conjugate or free c_{e6} (c_{e6} equivalent concentration of 4 nmol per well) and incubated for 3 h at 37°C. Immediately prior to illumination the cells were washed three times with PBS with Mg++/Ca++, the wells were replenished with 1 mL medium containing HEPES and 10% FCS. A 660 nm light was delivered from beneath the wells from a diode laser at a fluence rate of 50 mW cm^{-2} *via* a fiber optic–coupled microscope objective. Wells were illuminated in blocks of four defined by a black mask placed beneath the 24-well plate. Fluences were 2, 5 and 10 J cm^{-2}. After completion of illumination, the dishes were returned to the incubator for a further 24 h incubation. Cell survival was determined by the 3-(4,5-dimethylthiazol-2-yl)-2,5-diphenyltetrazolium bromide (MTT) assay, which measures mitochondrial dehydrogenase activity. It has been extensively used for measuring viability of cell cultures after PDT and has been shown to have close correlation with colony forming assays (35). Twenty-four

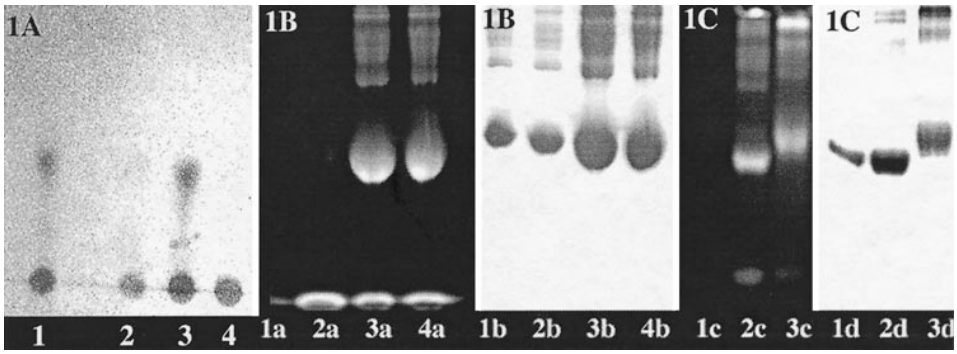

Figure 1. TLC and PAGE. (A) TLC developed in a 1:1 mixture of 10% aqueous ammonium chloride and methanol. Lane 1: single peak of BSA–c_{e6} isolated from Sephadex G50 column; lane 2: same as lane 1 after four acetone precipitation steps; lane 3: crude mal-BSA–c_{e6}; lane 4: mal-BSA–c_{e6} after three acetone precipitation steps. (B) and (C) SDS-PAGE (4–10% gradient) visualized by fluorescence imaging (lanes 1a–4a and 1c–3c) and Coomassie blue staining (lanes 1b–4b and 1d–3d). (B) Lanes 1a and 1b: BSA; lanes 2a and 2b: mixture of BSA with free c_{e6}; lanes 3a and 3b single peak from Sephadex G50 column purification of BSA–c_{e6} 1; lanes 4a and 4b: single peak from Sephadex G50 column purification of mal-BSA–c_{e6}. (C) Lanes 1c and 1d: BSA; lanes 2c and 2d: BSA–c_{e6} 1 after three acetone precipitation steps; lanes 3c and 3d: mal-BSA–c_{e6}, 2 after three acetone precipitation steps.

hours after illumination, the cells were given fresh media and 100 μL MTT (5 mg mL^{-1}) solution was added to each well and cells were incubated at 37°C. After 1 hour incubation the supernatant medium was gently aspirated and 1 mL of DMSO was added to lyse the cells and dissolve the deep-blue formazan. Plates were gently shaken on an orbital shaker in the dark for 15 min to complete the dissolution of any formazan crystals and the blue DMSO solution was transferred to 96-well plates (200 μL per well, 5 wells per well of 24-well plate). Absorbance was read on an automated plate reader (Model 2550 EIA, Bio-Rad Laboratories, Hercules, CA) at 570 nm. Data points were the average of 3 wells of the 24-well plate (15 wells of 96-well plate).

Competition. The role of scavenger receptors in the uptake of these conjugates was tested by measuring the reduction in the cellular content of PS produced by competing the uptake with a ligand known to be recognized by the scavenger receptor. The reduction in cellular uptake was then related to protection of the cells from phototoxicity. Increasing amounts of unlabeled mal-BSA were added simultaneously with the conjugates to J774 and OVCAR-5 cells and incubated for 3 h. About 0, 50, 100 and 200 μg mL^{-1} mal-BSA were used, representing a range of 0.25–3-fold molar excesses of the BSA contained in 4 μ*M* BSA–c_{e6} or mal-BSA–c_{e6}. The cellular uptakes and phototoxicities were measured as described above.

Confocal microscopy. The red intracellular fluorescence from c_{e6} was imaged in the cells together with simultaneous addition of either a mitochondrial green fluorophore, rhodamine 123 (R123, Eastman Kodak, Rochester, NY) or a lysosomal green fluorophore, Lysotracker® (Molecular Probes, Eugene, OR) in order to determine the subcellular organelle(s) which accumulate the c_{e6}. Square glass coverslips (22 × 22 mm^2) were put into 5 cm Petri dishes, and 5 × 10^5 cells in 4 mL medium were seeded in each dish and allowed to attach and grow on the coverslips until they formed a monolayer, which was 60–70% confluent. Conjugates were added at a final concentration of 2 μ*M* and allowed to incubate in serum-containing medium for 3 h. For the final 30 m, sufficient R123 or Lysotracker to make the concentration in the final medium 25 n*M* was added. The solutions were then aspirated from the dishes, washed three times with PBS and the coverslips removed, mounted on a histological slide in PBS and examined with a laser scanning confocal fluorescence microscope. A Leica DMR confocal laser fluorescence microscope (Leica Mikroskopie und Systeme GmbH, Wetzler, Germany) (excitation 488 nm argon laser) and a 100× oil immersion objective was used to image at a resolution of 1024 × 1024 pixels. Two channels collected fluorescence signals in either the green range (580 nm dichroic mirror plus 530 nm [±10 nm] bandpass filter) or the red range (580 nm dichroic mirror plus 590 nm longpass filter) and were displayed as false color images. These channels were overlaid using TCS NT software (Version 1.6.551, Leica Lasertechnik, Heidelberg, Germany) to allow visualization of overlap of red and green fluorescence.

RESULTS

Preparation and purification of conjugates

A significant problem encountered in the preparation of covalent conjugates of tetrapyrrole PS with proteins is the tendency of the dye to form tightly bound noncovalent complexes as well as conjugates. This has been reported in the literature previously (36). These mixtures can be difficult to separate into pure conjugate and nonbound dye. This is illustrated by the attempted use of a Sephadex G50 column to separate the BSA–c_{e6} conjugate from unreacted c_{e6}–NHS ester and its subsequent reaction products. Monitoring of the eluted fractions at 400 and at 280 nm showed a single peak that contained both the c_{e6} and the protein. However when the material obtained from combining the fractions was examined by TLC, as shown in Fig. 1A, it is apparent that there was a considerable amount of unbound dye present. Lane 1 on the TLC shows the single peak isolated from the size exclusion column and demonstrates that there is still considerable unbound c_{e6} present as a fast running spot. When this material was used in cell-uptake experiments, it was impossible to demonstrate any receptor targeting between J774 and OVCAR-5 cells (data not shown). The reason is the contaminating c_{e6} derivatives appear to be lipophilic and are taken up indiscriminately by both receptor-positive and receptor-negative cells. Likewise, lane 3 shows the crude mixture after maleylation and that there is unbound c_{e6} also present.

We therefore developed a novel means of purifying the conjugates, using acetone precipitation, that allowed the lipophilic c_{e6} species to be retained in the acetone supernatant and the precipitated conjugates to be redissolved in a purified form. The SDS-PAGE gels can be viewed by fluorescence imaging to localize the c_{e6} by the red fluorescence, and after staining with Coomassie Blue the protein can be localized. Figure 1B shows corresponding fluorescence and Coomassie images of BSA, BSA mixed with free c_{e6}, and conjugates (BSA–c_{e6} 1 and mal-BSA–c_{e6} 1) after Sephadex column chromatography but before acetone precipitation. The mixture of BSA and c_{e6} (lanes 2a and 2b) shows that no fluorescence is retained by the protein band on the gel, thus

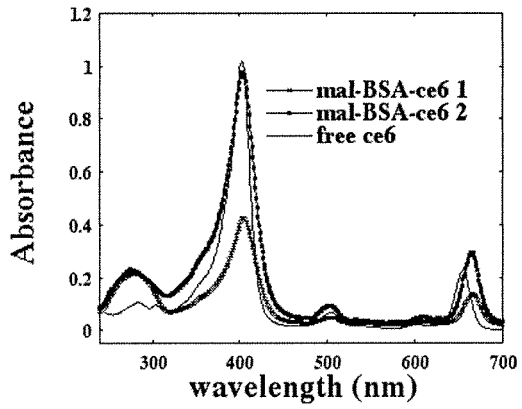

Figure 2. UV–visible absorption spectra. Mal-BSA–c_{e6} 1 and 2 were dissolved in 0.1 *M* NaOH/1% SDS to give solutions with concentrations of protein = 150 μg mL^{-1} (2.24 μ*M*), free c_{e6} was dissolved in 0.1 *M* NaOH/1% SDS to give a concentration of 6.5 μ*M*.

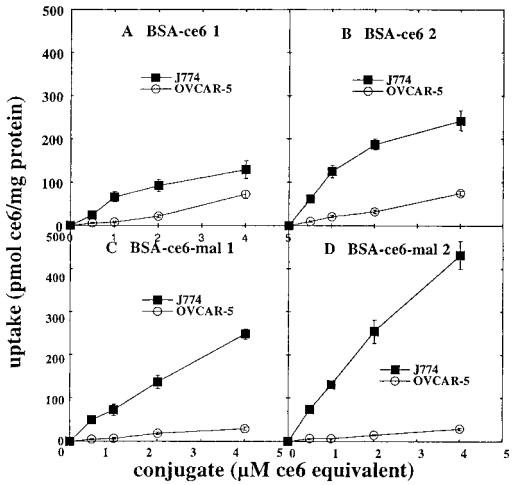

Figure 3. Cellular uptake of c_{e6} from conjugates. Conjugates (A: BSA–c_{e6} 1; B: BSA–c_{e6} 2; C: mal-BSA–c_{e6} 1; D: mal-BSA–c_{e6} 2) were incubated for 3 h in serum-containing medium at 37°C with either J774 or OVCAR-5 cells. Cells were then extracted with 0.1 *M* NaOH/1% SDS for 24 h to give homogeneous solutions. Fluorescence was measured and c_{e6} content was quantified by comparison with calibration curves prepared for each conjugate. Values are means from three wells and bars are SE.

demonstrating that a fluorescent band localizing with the protein is evidence of covalent conjugation. The lanes of the conjugates (3a and 3b; 4a and 4b) both show that a fluorescent band running at the gel front, remains after Sephadex chromatography.

The efficiency of the purification by acetone precipitation of the conjugates is confirmed by the gel electrophoresis images shown in Fig. 1C. It can be seen that the fast running fluorescent band has disappeared from both the BSA–c_{e6} and the mal-BSA–c_{e6} (lanes 2c and 2d; 3c and 3d), while the TLC also shows the disappearance of the fast running spot (Fig. 1A, lanes 2 and 4)

The UV–visible absorption spectra of the purified mal-BSA–c_{e6} conjugates with the two substitution ratios measured at equal protein concentrations are shown in Fig. 2 together with free c_{e6} at approximately the same concentration as is present in mal-BSA–c_{e6} 2. Similar spectra were obtained for BSA–c_{e6} 1 and 2 (data not shown). Using the values for molar extinction coefficients of BSA at 280 nm of 47 000 cm^{-1} M^{-1} (32) and c_{e6} at 400 nm of 150 000 cm^{-1} M^{-1} and correcting for the small absorbance of c_{e6} at 280 nm, the substitution ratios can be calculated to be mal-BSA–c_{e6} 1 ratio = approximately 1 protein to 1 dye, and mal-BSA–c_{e6} 2, ratio = approximately 1 protein to 3 dye.

Cellular uptake and phototoxicity

These conjugates show remarkable cell type specificity for macrophages compared to ovarian cancer cells both in uptake and in phototoxicity. This selectivity is especially evident when care has been taken to remove all non–covalently bound c_{e6} as described above. In the case of the J774 cells the amount of c_{e6} removed from the cells by the trypsin was less than 10% of the value extracted from the cells after trypsin incubation, but in the case of the OVCAR-5 cells, although the amounts in the trypsin were slightly less than those found with the J774 cells, this value was comparable with the amount extracted (data not shown). The data (Fig. 3a–d) show the uptake after 3 h incubation in 10% serum-containing medium by J774 cells and OVCAR-5 cells. Four conjugates were used: BSA–c_{e6} 1 and mal-BSA–c_{e6} 1 had a 1:1 molar ratio of BSA:c_{e6}, while BSA–c_{e6} 2 and mal-BSA–c_{e6} 2 had a 1:3 ratio. The molar ratios were identical for maleylated and nonmaleylated conjugates because one was prepared from the other. The c_{e6} uptake by J774 cells from BSA–c_{e6} 2 is greater than from BSA–c_{e6} 1 and similarly the uptake from mal-BSA–c_{e6} 2 is greater than from mal-BSA–c_{e6} 1. The c_{e6} uptake by J774 cells from the maleylated conjugate is greater than from the corresponding nonmaleylated conjugate, but interestingly the reverse is the case for OVCAR-5 cells. In both cases the uptake by OVCAR-5 cells is higher from the nonmaleylated conjugate than from the maleylated derivative. For these reasons the selectivity for J774 cells compared to OVCAR-5 cells increases in the order BSA–c_{e6} 1 < BSA–c_{e6} 2 < mal-BSA–c_{e6}1 < mal-BSA–c_{e6} 2.

The graphs shown in Fig. 4a–d compare the phototoxicity found for the two cell lines after a 3 h incubation in 10% serum-containing medium with 4 μ*M* c_{e6} equivalent concentration of the four conjugates. There was no phototoxicity seen in the OVCAR-5 nontarget cells with any conjugate. For the target J774 cells the order of phototoxicity was mal-BSA–c_{e6} 2 > BSA–c_{e6} 2 > mal-BSA–c_{e6} 1 > BSA–c_{e6} 1. At 10 J cm^{-2} after incubation with mal-BSA–c_{e6} 2 the fraction of J774 cells that were killed was more than two log values higher than that for OVCAR-5 cells.

It is accepted that active uptake by processes such as fluid phase endocytosis, receptor-mediated endocytosis and phagocytosis are all substantially reduced or abolished by lowering the temperature of the incubation to 4°C (37). By comparing uptake at 4°C with that at 37°C for varying conjugates, the proportion of each uptake due to active endocytosis can be determined. Table 1 shows the ratios of the uptake at 4°C to the uptake at 37°C. It can be seen that for J774 cells and BSA–c_{e6} 1 and 2 the ratios are similar at 0.46 and 0.44, respectively, while the ratios for mal-BSA–c_{e6} 1 and 2 are significantly lower at 0.23 and 0.14, respectively. However the situation is completely different for OVCAR-5 cells where all the ratios are significantly greater than 1,

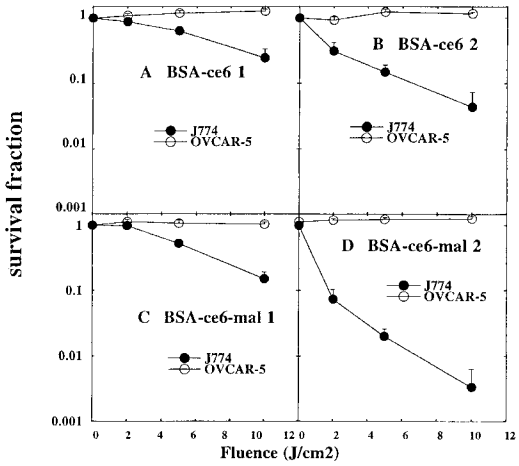

Figure 4. Phototoxicity. After cells had been incubated with conjugates (A: BSA–c_{e6} 1; B: BSA–c_{e6} 2; C: mal-BSA–c_{e6} 1; D: mal-BSA–c_{e6} 2) at 4 μM c_{e6} equivalent concentration for 3 h in serum-containing medium at 37°C, they received 660 nm light at a fluence rate of 50 mW cm^{-2}. Survival fractions were determined 24 h later by MTT colorimetric assay. Values are means of three wells of 24-well plates (15 wells of 96-well plate) and bars are SE.

and the ratios for mal-BSA–c_{e6} 1 and 2 (3.57 and 5.01, respectively) are significantly higher than those for BSA–c_{e6} 1 and 2 (1.73 and 1.94, respectively).

Competition

The data shown in Fig. 5a–d show the effect of competing the uptake of conjugates, and protecting against phototoxicity in J774 cells by adding increasing amounts of unlabeled mal-BSA. The same conditions were used for all incubations, *i.e.* 4 μM c_{e6} equivalent incubation carried out for 3 h at 37°C in serum-containing medium, and 10 J cm^{-2} light fluence. There was no effect of adding mal-BSA on the uptake or phototoxicity of OVCAR-5 cells (data not shown). In these plots it can be seen that the proportion of uptake competed and the proportion of phototoxicity protected against is higher for the maleylated conjugates and also appears to be slightly greater for the conjugates with the high substitution ratio. The competition against the maleylated conjugates is also more pronounced at lower mal-BSA concentrations (50 μg mL^{-1}).

Confocal microscopy

The use of green fluorescing probes specific for subcellular organelles provides valuable information on the intracellular localization of the red c_{e6} fluorescence delivered into the cells by the conjugates. Cells were incubated with 2 μM c_{e6} equivalent for 3 h in serum-containing medium. As expected from the extremely low uptake of c_{e6} found with OVCAR-5 cells, Fig. 6c,d,g,h shows very little red signal, and the mitochondrial probe R123 gives a stronger green signal (Fig. 6d,h) than the lysosomal probe (Fig. 6c,g), indicating that OVCAR-5 cells have more pronounced mitochondria than lysosomes. In contrast the J774 macrophages show a much higher red signal (Fig. 6a,b,e,f), and the red fluorescence shows a high degree of overlap with the green lysosomal probe (Fig. 6a,e) while the red and green are notably distinct in the case of the mitochondrial probe (Fig. 6b,f). Note that there is more red fluorescence taken up by J774 cells from the maleylated conjugate (Fig. 6e,f) than the nonmaleylated conjugate (Fig. 6a,b); this is consistent with the higher measured uptake of c_{e6} from the mal-BSA–c_{e6}. These data confirm that the conjugates are taken up and internalized by J774 cells into lysosomes, while the low uptake of OVCAR-5 cells does not allow any firm conclusion to be reached about intracellular localization.

Table 1. Ratios of uptakes of c_{e6} at 4°C to that at 37°C from conjugates*

	J774	OVCAR-5
BSA–c_{e6} 1	0.46 ± 0.02	1.73 + 0.26
BSA–c_{e6} 2	0.44 ± 0.06	1.94 + 0.28
Mal-BSA–c_{e6} 1	0.23 + 0.03	3.57 + 0.19
Mal-BSA–c_{e6} 2	0.14 + 0.01	5.01 + 0.89

* The uptake of the conjugates was measured after incubation for 3 h in serum-containing medium at either 4 or 37°C. The concentrations were 0.5, 1, 2 and 4 μM c_{e6} equivalent, and ratios were taken of the 4 or 37°C uptake (expressed in pmol c_{e6} equivalent per mg cell protein) at each concentration. Values are the mean ± SE of the four ratios for each cell line and conjugate.

DISCUSSION

The use of protein–PS conjugates to obtain cell type–specific targeting may constitute an improvement in PS delivery in PDT. One way of achieving this goal is the covalent attachment of PS to ligands of the macrophage scavenger receptor, this approach has previously been reported by us (12,13) and others (20,22). In this report we have shown that purification of the albumin conjugates in order to remove unbound lipophilic c_{e6} species allows specific targeting of receptor-positive J774 macrophages, with essentially no phototoxicity toward the receptor-negative OVCAR-5 cancer cells. It was found that when the conjugates with differing substitution ratios were added at the same concentration of c_{e6} equivalent

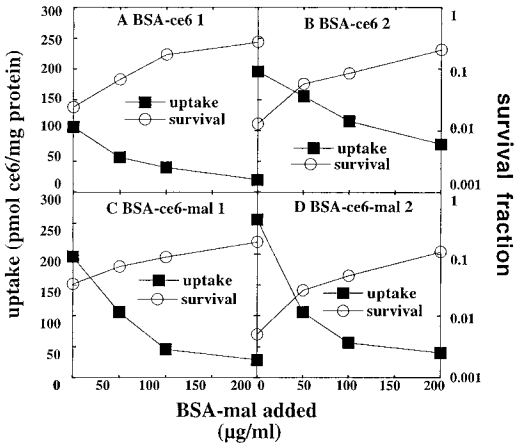

Figure 5. Competition of uptake and protection from phototoxicity. Cells were incubated with conjugates (A: BSA–c_{e6} 1; B: BSA–c_{e6} 2; C: mal-BSA–c_{e6} 1; D: mal-BSA–c_{e6} 2) at 4 μM c_{e6} equivalent concentrations with increasing amounts of mal-BSA added simultaneously; c_{e6} uptake and phototoxicity were determined as described earlier.

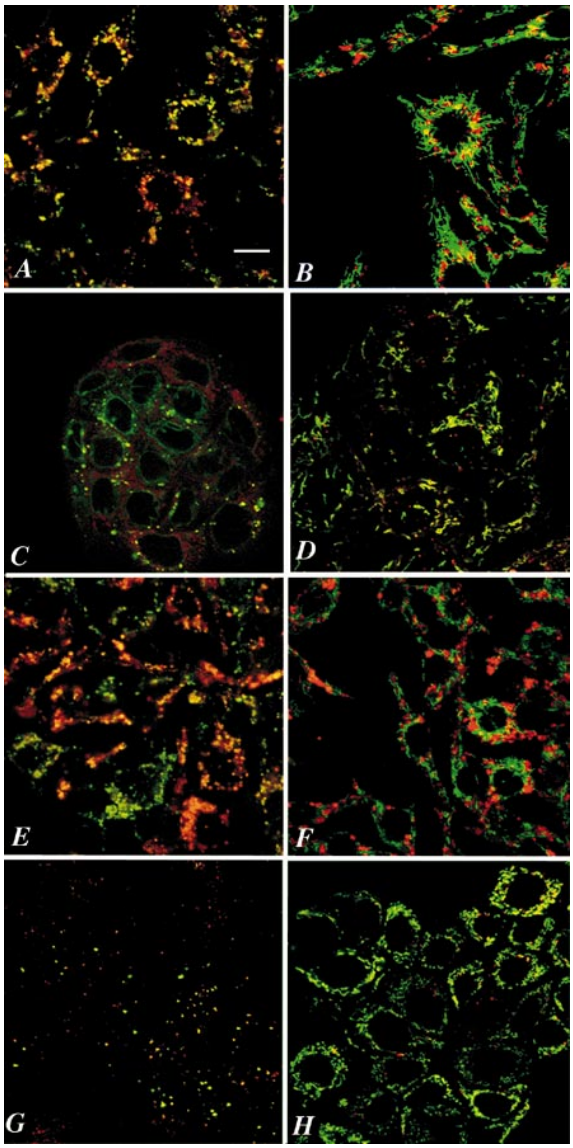

Figure 6. Confocal micrographs. Cells were grown on coverslips and incubated with conjugates (2 μ*M* c_{e6} equivalent concentration) for 3 h and for the last 30 min with R123 or Lysotracker (25 n*M*). A Leica laser scanning confocal microscope was used to generate images with either red (590+ nm) or green (520–540 nm) fluorescence and these were overlaid to produce the two-color images. A–D, BSA–c_{e6} 2; E–H, mal-BSA–c_{e6} 2; A,B,E,F, J774 cells; C,D,G,H, OVCAR-5 cells; A,C,E,G, Lysotracker; B,D,F,H, R 123.

(this means that three times as much protein was added in the case of BSA–c_{e6} 1 as in BSA–c_{e6} 2), the uptake of c_{e6} was two-fold higher for the conjugates with the higher substitution ratios. The uptake *versus* concentration curves showed signs of becoming saturated in the case of J774 cells and BSA–c_{e6} 1 and 2 but not for the mal-BSA–c_{e6} conjugates. Since the number of conjugate molecules present in the medium was three times higher for the low substitution ratio (because the concentrations were specified in terms of c_{e6} equivalent), if the affinities and rates of uptake by the cells were similar, one would have expected equal cellular uptakes of c_{e6} from the two substitution ratios. However, if the concentration of conjugates in the medium were sufficient to saturate the receptors, then one would expect that the cellular uptake would be independent of the concentration in the medium and the uptake would be three times higher for the conjugates with the higher substitution ratios, but this saturation is not likely as can be seen from the curves in Fig. 3. It is also possible that an albumin conjugate that has had its structure more modified by attaching three c_{e6} molecules rather than one has tighter binding to the receptor and hence a higher uptake. The uptake by J774 cells of c_{e6} from the maleylated conjugate was almost twice that from the nonmaleylated precursor for both substitution ratios. This finding is additional evidence for the hypothesis that increased alteration of the serum albumin increases the recognition by the receptor and hence the uptake.

Non–scavenger receptor–expressing OVCAR-5 cells took up significantly more c_{e6} from nonmaleylated conjugates than from their maleylated counterparts. In addition the uptake of BSA–c_{e6} 1 and 2 by OVCAR-5 cells did not show the saturation seen with the uptake by J774 cells. The explanation for these observations is not clear. The phototoxicity towards J774 cells as shown in Fig. 5 was mainly in line with the cellular uptake of c_{e6}. The complete lack of phototoxicity toward the OVCAR-5 cells even though there was some significant uptake, especially in the case of the nonmaleylated conjugates, might be explained by the greater ability of the J774 cells to hydrolyze these conjugates once taken up into lysosomes. If these macromolecular conjugates become significantly more phototoxic when broken down into small fragments to release the free more photoactive dye, as has been reported by Krinick *et al.* (38), the macrophages are ideally suited to this task. However, it should be noted that even if the conjugates are broken down releasing free PS into the lysosomes, the lysosomal localization of the PS is likely to be significantly less efficient (per molecule of PS) in killing the cells than other intracellular localizations such as the mitochondria.

The competition experiments showed that the uptake and phototoxicity of both the maleylated and nonmaleylated conjugates toward the J774 cells could be competed by an archetypal scavenger receptor ligand. However the competition was more effective against mal-BSA–c_{e6} 1 and 2 than the nonmaleylated precursors. It also appears that the competition was more effective against the conjugates with higher substitution ratios. The explanation for these observations is presumably that there are at least two recognition sites for these conjugates. The more highly altered albumin molecules are mainly recognized by the scavenger receptor, while the less altered albumin molecules are also recognized by another receptor.

In a recent publication Brasseur *et al.* (20) described the preparation and phototoxicity of series of conjugates between BSA or mal-BSA and the PS aluminum phthalocyanine tetrasulfonate. They used J774 cells and a non–scavenger receptor–expressing murine cancer cell line EMT-6. They did not directly measure the uptake of PS by the cells, but found some degree of selective phototoxicity toward the macrophage cell line. In agreement with the present study the maleylated conjugates had higher phototoxicity than their nonmaleylated counterparts. Nagae *et al.* (22) reported on the use of a conjugate between mal-BSA and c_{e6} to target intimal hyperplasia *in vivo*. They found that the mal-BSA–

c_{e6} gave significant fluorescence localization in lesions and good PDT treatment response compared to free c_{e6}.

Recently, the role of scavenger receptors in many physiological processes such as atherogenesis (16), defense against pathogens (39) and phagocytosis of apoptotic cells (40) has been appreciated; however the precise structural requirements needed for receptor ligand recognition are less clear. The wide and seemingly unrelated range of structures recognized by these receptors has led to them being termed ''molecular flypaper'' (41). The ligands are all macromolecules with a pronounced anionic charge but additional conformational factors are clearly involved (42) and the precise determinants of recognition are incompletely understood (43). Because of the specificity, high capacity and efficient routing to lysosomes for degradation by proteases, the use of covalent conjugates between scavenger receptor ligands and various drugs to produce macrophage-targeted therapy has been investigated. Basu and co-workers (44,45) have demonstrated this principle in targeting J774 and other macrophage-like cells *in vitro* with conjugates between maleylated albumin and daunorubicin. They showed that with J774 cells growing as tumors *in vivo* there was a significant response with the conjugate that was not seen with the same concentrations of free drug (19).

In contrast to previous theories (46), that TAM were ''fighting a valiant but losing battle against the malignant cells,'' it is now thought that the relationship between the tumor and the TAM is symbiotic in that both populations help each other to survive and grow in various ways (23). This relationship has been termed (47) a ''ping–pong reciprocal feeding interaction.'' Tumors actively recruit macrophages (48) and encourage their growth by expressing chemotactic molecules and growth factors for macrophages/monocytes (49). In return the TAM can help the tumor to grow and spread in four distinct ways. They can secrete paracrine growth factors for tumor cells (50), they can secrete proangiogenic factors to encourage the formation of neovasculature (51), they can produce proteases that degrade extracellular matrix and help local invasion and metastasis (52) and they can mediate immune suppression thus allowing the tumor to evade immune surveillance (53). For these reasons TAM have been proposed to be a ''target for cancer therapy'' (54). Macrophage-targeted PDT may be a good example of this approach as the ability to confine illumination to the tumor together with the cell type–specific targeting should allow the TAM to be killed while sparing other macrophage/monocyte subclasses in other locations. Experiments are underway in our laboratory to test these conjugates as targeted PDT agents against mouse tumors *in vivo.*

Acknowledgments—This work was funded by the ONR-MFEL program, Contract grant N 00014-94-1-0927. The authors gratefully acknowledge the support of Dr. Tayyaba Hasan, and thank Mark D. Savellano for helpful discussions, and Humayon B. Khan and David A. O'Donnell for technical assistance.

REFERENCES

1. Trail, P. A. and A. B. Bianchi (1999) Monoclonal antibody drug conjugates in the treatment of cancer. *Curr. Opin. Immunol.* **11**, 584–588.
2. Ennis, B. W., M. E. Lippman and R. B. Dickson (1991) The EGF receptor system as a target for antitumor therapy. *Cancer Investig.* **9**, 553–562.
3. Pasqualini, R., E. Koivunen and E. Ruoslahti (1997) Alpha v integrins as receptors for tumor targeting by circulating ligands. *Nature Biotechnol.* **15**, 542–546.
4. Eisenbrand, G., M. R. Berger, H. P. Brix, J. E. Fischer, K. Muhlbauer, M. R. Nowrousian, M. Przybilski, M. R. Schneider, W. Stahl, W. Tang, O. Zelezny and W. J. Zeller (1989) Nitrosoureas. Modes of action and perspectives in the use of hormone receptor affinity carrier molecules. *Acta Oncol.* **28**, 203–211.
5. Reddy, J. A. and P. S. Low (1998) Folate-mediated targeting of therapeutic and imaging agents to cancers. *Crit. Rev. Ther. Drug. Carrier Syst.* **15**, 587–627.
6. de Smidt, P. C. and T. J. van Berkel (1990) LDL-mediated drug targeting. *Crit. Rev. Ther. Drug Carrier Syst.* **7**, 99–120.
7. Hamblin, M. R. and E. L. Newman (1994) On the mechanism of the tumour-localising effect in photodynamic therapy. *J. Photochem. Photobiol. B: Biol.* **23**, 3–8.
8. Del Governatore, M., M. R. Hamblin, E. E. Piccinini, G. Ugolini and T. Hasan (2000) Targeted photodestruction of human colon cancer cells using charged 17.1A $chlorin_{e6}$ immunoconjugates. *Br. J. Cancer* **82**, 56–64.
9. Duska, L. R., M. R. Hamblin, J. L. Miller and T. Hasan (1999) Combination photoimmunotherapy and cisplatin: effects on human ovarian cancer ex vivo. *J. Natl. Cancer Inst.* **91**, 1557–1563. [See comments]
10. Duska, L. R., M. R. Hamblin, M. P. Bamberg and T. Hasan (1997) Biodistribution of charged F(ab′)2 photoimmunoconjugates in a xenograft model of ovarian cancer. *Br. J. Cancer* **75**, 837–844.
11. Hamblin, M. R., J. L. Miller and T. Hasan (1996) Effect of charge on the interaction of site-specific photoimmunoconjugates with human ovarian cancer cells. *Cancer Res.* **56**, 5205–5210.
12. Hamblin, M. R. and E. L. Newman (1994) Photosensitizer targeting in photodynamic therapy. II. Conjugates of haematoporphyrin with serum lipoproteins. *J. Photochem. Photobiol. B: Biol.* **26**, 147–157.
13. Hamblin, M. R. and E. L. Newman (1994) Photosensitizer targeting in photodynamic therapy. I. Conjugates of haematoporphyrin with albumin and transferrin. *J. Photochem. Photobiol. B: Biol.* **26**, 45–56.
14. Gijsens, A. and P. De Witte (1998) Photocytotoxic action of EGF-PVA-Sn(IV)$chlorin_{e6}$ and EGF-dextran-Sn(IV)$chlorin_{e6}$ internalizable conjugates on A431 cells. *Int. J. Oncol.* **13**, 1171–1177.
15. Akhlynina, T. V., A. A. Rosenkranz, D. A. Jans and A. S. Sobolev (1995) Insulin-mediated intracellular targeting enhances the photodynamic activity of $chlorin_{e6}$. *Cancer Res.* **55**, 1014–1019.
16. Freeman, M. W. (1997) Scavenger receptors in atherosclerosis. *Curr. Opin. Hematol.* **4**, 41–47.
17. Fukuda, S., S. Horiuchi, K. Tomita, M. Murakami, Y. Morino and K. Takahashi (1986) Acetylated low-density lipoprotein is endocytosed through coated pits by rat peritoneal macrophages. *Virchows Arch. B: Cell Pathol. Incl. Mol. Pathol.* **52**, 1–13.
18. Ding, Y., H. Hakamata, H. Matsuda, T. Kawano, T. Kawasaki, A. Miyazaki and S. Horiuchi (1998) Reduced expression of the macrophage scavenger receptors in macrophage-like cell mutants resistant to brefeldin A. *Biochem. Biophys. Res. Commun.* **243**, 277–283.
19. Mukhopadhyay, B., A. Mukhopadhyay and S. K. Basu (1993) Enhancement of tumouricidal activity of daunomycin by receptor-mediated delivery. *In vivo* studies. *Biochem. Pharmacol.* **46**, 919–924.
20. Brasseur, N., R. Langlois, C. La Madeleine, R. Ouellet and J. E. van Lier (1999) Receptor-mediated targeting of phthalocyanines to macrophages via covalent coupling to native or maleylated bovine serum albumin. *Photochem. Photobiol.* **69**, 345–352.
21. Takata, K., S. Horiuchi and Y. Morino (1989) Scavenger receptor-mediated recognition of maleylated albumin and its relation to subsequent endocytic degradation. *Biochim. Biophys. Acta* **984**, 273–280.
22. Nagae, T., A. Y. Louie, K. Aizawa, S. Ishimaru and S. E. Wilson (1998) Selective targeting and photodynamic destruction of

intimal hyperplasia by scavenger-receptor mediated protein–chlorin$_{e6}$ conjugates. *J. Cardiovasc. Surg. (Torino)* **39**, 709–715.
23. Mantovani, A. (1994) Tumor-associated macrophages in neoplastic progression: a paradigm for the *in vivo* function of chemokines. *Lab. Investig.* **71**, 5–16.
24. Harmey, J. H., E. Dimitriadis, E. Kay, H. P. Redmond and D. Bouchier-Hayes (1998) Regulation of macrophage production of vascular endothelial growth factor (VEGF) by hypoxia and transforming growth factor beta-1. *Ann. Surg. Oncol.* **5**, 271–278.
25. Leek, R. D., C. E. Lewis, R. Whitehouse, M. Greenall, J. Clarke and A. L. Harris (1996) Association of macrophage infiltration with angiogenesis and prognosis in invasive breast carcinoma. *Cancer Res.* **56**, 4625–4629.
26. Pupa, S. M., R. Bufalino, A. M. Invernizzi, S. Andreola, F. Rilke, L. Lombardi, M. I. Colnaghi and S. Menard (1996) Macrophage infiltrate and prognosis in c-erbB-2-overexpressing breast carcinomas. *J. Clin. Oncol.* **14**, 85–94.
27. Visscher, D. W., P. Tabaczka, D. Long and J. D. Crissman (1995) Clinicopathologic analysis of macrophage infiltrates in breast carcinoma. *Pathol. Res. Pract.* **191**, 1133–1139.
28. Korbelik, M. and G. Krosl (1996) Photofrin accumulation in malignant and host cell populations of various tumours. *Br. J. Cancer* **73**, 506–513.
29. Korbelik, M. and G. Krosl (1995) Photofrin accumulation in malignant and host cell populations of a murine fibrosarcoma. *Photochem. Photobiol.* **62**, 162–168.
30. Korbelik, M., V. R. Naraparaju and N. Yamamoto (1997) Macrophage-directed immunotherapy as adjuvant to photodynamic therapy of cancer. *Br. J. Cancer* **75**, 202–207.
31. Krosl, G., M. Korbelik, J. Krosl and G. J. Dougherty (1996) Potentiation of photodynamic therapy-elicited antitumor response by localized treatment with granulocyte-macrophage colony-stimulating factor. *Cancer Res.* **56**, 3281–3286.
32. Laemmli, U. K. (1970) Cleavage of structural proteins during the assembly of the head of bacteriophage T4. *Nature* **227**, 680–685.
33. Markwell, M. A., S. M. Haas, L. L. Bieber and N. E. Tolbert (1978) A modification of the Lowry procedure to simplify protein determination in membrane and lipoprotein samples. *Anal. Biochem.* **87**, 206–210.
34. McHale, A. P. and L. McHale (1988) Use of a tetrazolium based colorimetric assay in assessing photoradiation therapy *in vitro*. *Cancer Lett.* **41**, 315–321.
35. Feldhoff, R. C., M. C. Steffen, T. E. Geoghegan and B. E. Ledford (1985) Purification of trnsferrin and albumin from mouse ascites fluid. *Prep. Biochem.* **15**, 221–236.
36. Mew, D., C. K. Wat, G. H. Towers and J. G. Levy (1983) Photoimmunotherapy: treatment of animal tumors with tumor-specific monoclonal antibody-hematoporphyrin conjugates. *J. Immunol.* **130**, 1473–1477.
37. Silverstein, S. C., R. M. Steinman and Z. A. Cohn (1977) Endocytosis. *Ann. Rev. Biochem.* **46**, 669–722.
38. Krinick, N. L., Y. Sun, D. Joyner, J. D. Spikes, R. C. Straight and J. Kopecek (1994) A polymeric drug delivery system for the simultaneous delivery of drugs activatable by enzymes and/or light. *J. Biomater. Sci. Polym. Ed.* **5**, 303–324.
39. Krieger, M. (1997) The other side of scavenger receptors: pattern recognition for host defense. *Curr. Opin. Lipidol.* **8**, 275–280.
40. Savill, J. (1997) Recognition and phagocytosis of cells undergoing apoptosis. *Br. Med. Bull.* **53**, 491–508.
41. Krieger, M. (1992) Molecular flypaper and atherosclerosis: structure of the macrophage scavenger receptor. *Trends Biochem. Sci.* **17**, 141–146.
42. Haberland, M. E. and A. M. Fogelman (1985) Scavenger receptor-mediated recognition of maleyl bovine plasma albumin and the demaleylated protein in human monocyte macrophages. *Proc. Natl. Acad. Sci. USA* **82**, 2693–2697.
43. Andersson, L. and M. W. Freeman (1998) Functional changes in scavenger receptor binding conformation are induced by charge mutants spanning the entire collagen domain. *J. Biol. Chem.* **273**, 19 592–19 601.
44. Basu, S. K. (1990) Receptor-mediated endocytosis of macromolecular conjugates in selective drug delivery. *Biochem. Pharmacol.* **40**, 1941–1946.
45. Mukhopadhyay, A., B. Mukhopadhyay, R. K. Srivastava and S. K. Basu (1992) Scavenger-receptor-mediated delivery of daunomycin elicits selective toxicity towards neoplastic cells of macrophage lineage. *Biochem. J.* **284**, 237–241.
46. van Ravenswaay Claasen, H. H., P. M. Kluin and G. J. Fleuren (1992) Tumor infiltrating cells in human cancer. On the possible role of CD16+ macrophages in antitumor cytotoxicity. *Lab. Investig.* **67**, 166–174.
47. Bottazzi, B., E. Erba, N. Nobili, F. Fazioli, A. Rambaldi and A. Mantovani (1990) A paracrine circuit in the regulation of the proliferation of macrophages infiltrating murine sarcomas. *J. Immunol.* **144**, 2409–2412.
48. Graves, D. T. and A. J. Valente (1991) Monocyte chemotactic proteins from human tumor cells. *Biochem. Pharmacol.* **41**, 333–337.
49. Zhang, L., A. Khayat, H. Cheng and D. T. Graves (1997) The pattern of monocyte recruitment in tumors is modulated by MCP-1 expression and influences the rate of tumor growth. *Lab. Investig.* **76**, 579–590.
50. O'Sullivan, C., C. E. Lewis, A. L. Harris and J. O. McGee (1993) Secretion of epidermal growth factor by macrophages associated with breast carcinoma. *Lancet* **342**, 148–149.
51. Torisu, H., M. Ono, H. Kiryu, M. Furue, Y. Ohmoto, J. Nakayama, Y. Nishioka, S. Sone and M. Kuwano (2000) Macrophage infiltration correlates with tumor stage and angiogenesis in human malignant melanoma: possible involvement of TNFalpha and IL-1alpha. *Int. J. Cancer* **85**, 182–188.
52. Hildenbrand, R., C. Jansen, G. Wolf, B. Bohme, S. Berger, G. von Minckwitz, A. Horlin, M. Kaufmann and H. J. Stutte (1998) Transforming growth factor-beta stimulates urokinase expression in tumor-associated macrophages of the breast. *Lab. Investig.* **78**, 59–71.
53. Elgert, K. D., D. G. Alleva and D. W. Mullins (1998) Tumor-induced immune dysfunction: the macrophage connection. *J. Leukoc. Biol.* **64**, 275–290.
54. Wahl, L. M. and H. K. Kleinman (1998) Tumor-associated macrophages as targets for cancer therapy. *J. Natl. Cancer Inst.* **90**, 1583–1584.